ISSN 0208-7774 TRIBOLOGIA 1/2022 p. 83–95
DOI: 10.5604/01.3001.0015.8987

Krzysztof WIERZCHOLSKI[*], Jacek GOSPODARCZYK[**]

ON THE IMPORTANT MEANING OF BIO-LIQUID DYNAMIC VISCOSITY VARIATIONS IN THE LUBRICATION FLOWS

O WAŻNYM ZNACZENIU ZMIAN LEPKOŚCI DYNAMICZNEJ CIECZY BIOLOGICZNEJ W PRZEPŁYWACH SMARUJĄCYCH

Key words: bio-liquid dynamic viscosity variations, experimental measurements, human hip joint, human joint diseases and bio-liquid dynamic viscosity, lubrication of bio-surfaces, physical parameters of bio-surface.

Abstract: The main topic of this paper refers to the numerous relations between the decrements of the dynamic viscosity of non-Newtonian bio-liquid lubricated human joints on the one hand and, on the other hand, with consequences resulting from various diseases such as low fitness and low skills of human limbs, joint unfitness, large wear of cooperating cartilage bio-surfaces. Additionally, this paper indicates the pharmacology methods performed in vivo to enhance the bio-liquid lubricant dynamic viscosity. After numerous experimental measurements, it directly follows that the collagen fibre, hyaluronate acid particle, power hydrogen ion concentration pH in lubricating bio-liquid and absorbability features of lubricated bio-surface have a direct and indirect significant influence on the bio-liquid dynamic viscosity values variations with interfacial energy distribution across the film thickness. The results presented in this paper are confirmed based on experimental measurements and analytical, numerical solutions of the load-carrying capacity, friction coefficient and bio-liquid dynamic variations performed for various human joints. These effects were simply disregarded in previous studies. The aforementioned problem has not been considered in contemporary research literature in the medical tribology domain to the Author's best knowledge. The results obtained should enable one to introduce more effective and accurate therapeutic protocols into the human joint treatment regimen. The results obtained have applications on a wide scale in spatiotemporal models in bio-tribology, biology and health science.

Słowa kluczowe: zmiany lepkości dynamicznej powierzchni biologicznej, pomiary eksperymentalne, staw biodrowy człowieka, choroby stawów człowieka a lepkość dynamiczna biocieczy, smarowanie biopowierzchni, parametry fizyczne powierzchni biologicznej.

Streszczenie: Główny temat pracy dotyczy licznych związków pomiędzy spadkiem lepkości dynamicznej nienewtonowskiej biocieczy smarującej stawy człowieka z jednej strony a konsekwencjami powodowanymi przez różne choroby z drugiej strony, takimi jak: mała sprawność oraz zręczność kończyn, brak sprawności stawów, znaczne zużycie powierzchni chrząstki.

Niniejsza praca przedstawia dodatkowo farmakologiczne metody powiększania in vivo lepkości dynamicznej smarującej cieczy biologicznej. Z licznych eksperymentalnych pomiarów wynika, że włókna kolagenowe, cząsteczki kwasu hialuronowego, potęgowa koncentracja jonów wodorowych pH w biologicznej cieczy smarującej oraz właściwości absorbcji smarowanej powierzchni chrząstki, mają istotny pośredni i bezpośredni wpływ na zmiany lepkości dynamicznej oraz rozkład energii wewnętrznej w poprzek grubości warstwy cieczy biologicznej. Przedstawione w pracy rezultaty potwierdzone zostały na podstawie eksperymentalnych pomiarów oraz analityczno-numerycznych obliczeń siły nośnej, współczynnika tarcia, zmian lepkości dynamicznej smarującej cieczy biologicznej, przeprowadzonych dla różnych stawów człowieka. We wcześniejszych badaniach takie efekty były pomijane. Według informacji autorów, rozpatrywany problem nie był rozpatrywany we współczesnych badaniach literaturowych tribologii medycznej. Przedstawione rezultaty umożliwią wykonywanie bardziej dokładnych leczniczych protokołów w trakcie wykonywania zabiegów dla stawów człowieka. Wyniki uzyskane w pracy znajdują zastosowanie na szeroką skalę w czasowo-przestrzennych modelach biotribologii oraz nauki o zdrowiu.

[*] ORCID: 0000-0002-9074-4200. University of Economy (WSG), Garbary 2 Street, 85-229 Bydgoszcz, Poland, e-mail: krzysztof.wierzcholski@wp.pl.

[**] ORCID: 0000-0001-8248-9329. University of Economy (WSG), Garbary 2 Street, 85-229 Bydgoszcz, Poland, e-mail: jacek.gospodarczyk@byd.pl.

INTRODUCTION

The results of the latest numerous bio-tribology studies, carried out by the means of new measurement devices, have demonstrated that the PL (phospholipid) layer and random gap height variations fairly significantly control the bio-liquid dynamic viscosity during the lubrication of cartilage surfaces **[L. 1–2]**.

The bio-lubricant flows in the joint gap, confined between two cartilage surfaces. During the bio-lubrication flow in the human joint gap, the superficial cartilage layer and the movable PL bilayer alter the bio-lubricants dynamic viscosity **[L. 3–5]**. We considered the structure of cartilage joints because the cartilage presents the most excellent sliding bearing material applied to human joints produced during many numerous thousands of years of evolution.

Joint cartilage (glassy) possesses no blood or lymphatic vessels; it is not innervated and is characterised by slow metabolism. In the case of injury, it has no possibility of idiopathic healing. Fibrous cartilage fillings do not remove defects. Fibrous cartilages are not resistant to compression because irregular and non-fit collagen fibres occur and dominate in this medium. The properties of regenerate cartilage significantly deviate in comparison with the sound cartilage of the human joint. The joint cartilage matrix presents a nonhomogeneous, hyper-elastic, anisotropic composite material consisting of the following components: ● cartilage cells, i.e. chondrocytes,● cells aggregates of proteo-glycans, ● collagen fibres. Chondrocytes have 10–30 μm (1 μm = 0.000 001 m) in size, they do not contact mutually, they comprise cartilage volume that is smaller by about 1.0%, cf. **Fig. 1a**. The chondrocyte cell is covered by the fibre matrix of chondroid presented in **Fig. 1b**. Chondroid is a molecular bio-bag, which includes three or four or five chondrocytes **[L. 6–7]**.

One cubic millimetre of sound cartilage contains from 14,000 to 15,000 chondrocytes **Fig. 1c**. An average cross-section of the chondrocyte cell in a newborn baby has a value of 90 [μm^2], and it increases to about 370 [μm^2] in an adult. The chondrocyte has a large cell nucleus placed almost in the cell's centre (research by K. Wierzcholski **MTKDCT 517226**).

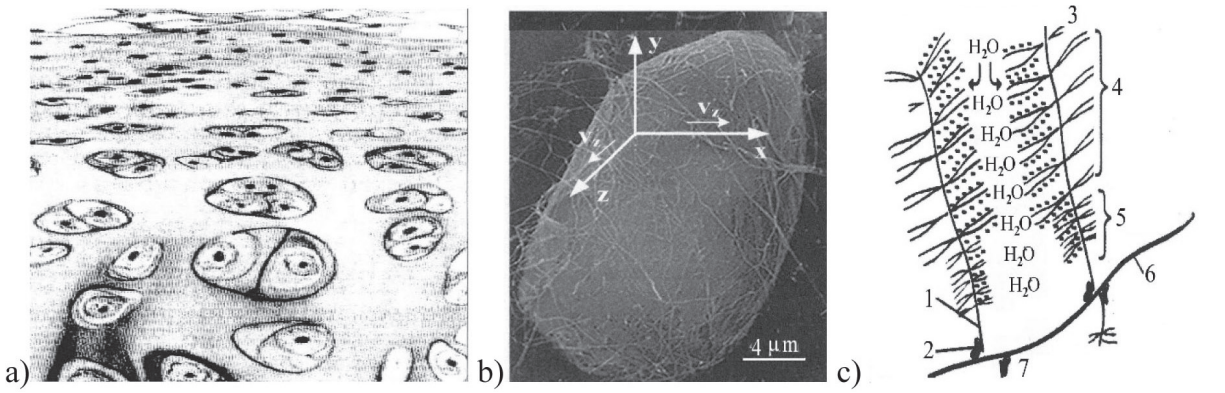

Fig. 1. Structure of joint cartilage: a) chondrocytes embedded in cartilage, b) photo of chondrocyte cell, c) aggregates cells of proteoglycans, (measurements are performed using the Atomic Force Microscope AFM); Notations: 1 – core protein, 2 – connection protein, 3 – amino – glycans, 4 – sulphate of chondroitin, 5 – sulphate of creatine, 6 – hyaluronic acid, 7 – proteoglycan aggregate

Rys. 1. Budowa chrząstki stawowej: a) chondrocyty wtopione w chrząstce, b) fotografia chondrocytu, c) agregat proteoglikanowy (pomiary wykonano przy użyciu mikroskopu sił atomowych AFM); Oznaczenia: 1 – białko rdzenia, 2 – białko łączące, 3 – glikozoaminoglikany, 4 – siarczan chondroityny, 5 – siarczan kreatanu, 6 – kwas hialuronowy, 7 – agregat proteoglikanowy

In their native state, chondrocytes occur in **[L. 3**, **8]** 1. The umbilical cord, 2. Human Bone Marrow. The amount of chondrocytes gained from human marrow is very small, and it is not sufficient. The cartilage in a forty-year-old human joint loses chondrocyte cells. Therefore, we have been cultivating chondrocytes in bioreactors for 20 years (from 2003). After experiments were performed, we see that: 1. Human joints without chondrocytes in cartilage are inefficient, and bio-liquid has a low dynamic viscosity, 2. Chondrocytes give efficiency and ability to human joints.

The elasticity modulus of elastic cartilage identifies strength and resistance. For the hypo-

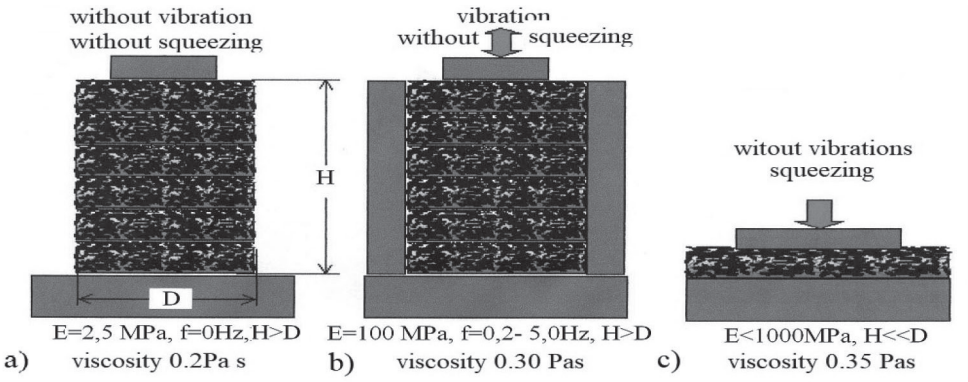

Fig. 2. Dynamic viscosity in Pas of bio-liquid between cartilage particles and elasticity modulus E in MPa of joint cartilage depends on squeezing load value P = 400 N and vibration frequency f < 5.0 Hz: a) E = 2.5 MPa, f = 0 Hz, P = 0 N, η = 0.2 Pas, b) E = 100 MPa, f = 0.2–5 Hz, P = 0 N, η = 0.30 Pas, c) E = 900 MPa, f = 0 Hz, P = 400 N, η = 0.35 Pas, (research results from K. Wierzcholski MTKDCT 2004 517226)

Rys. 2. Lepkość dynamiczna w Pas dla biocieczy pomiędzy jej cząsteczkami oraz moduł sprężystości E w MPa dla chrząstki stawowej zależny od siły wyciskania o wartości P = 400 N oraz od częstotliwości drgań f < 5,0 Hz: a) E = 2,5 MPa, f = 0 Hz, P = 0 N, η = 0,2 Pas, b) E = 100 MPa, f = 0,2–5 Hz, P = 0 N, η = 0,30 Pas, c) E = 900 MPa, f = 0 Hz, P = 400 N, η = 0,35 Pas (badania K.Wierzcholski grantu MTKDCT 2004 517226)

elastic properties of cartilage, many kinds of elasticity moduli have no consistent values. If the elasticity modulus of cartilage increases, then the strength of the cartilage increases **[L. 9–10]**. The aforementioned elasticity modulus of cartilage, bio-lubricant dynamic viscosity and friction forces are mutually connected during the lubrication process presented in **Fig. 2.**

The elasticity modulus of the cartilage identifies and is connected with the dynamic viscosity of the internal bio-liquid flow. Bio-liquid viscosity is created by friction and forces between mutually contacted cartilage particles during the squeezing process. If the friction force in the internal bio-liquid between the mutually contacted cartilage particles increases by squeezing, the cartilage's elasticity modulus and the bio-liquid's dynamic viscosity increase, see **Fig. 2a**, **2c**.

For example, after numerous performed measurements illustrated in **Fig. 2a** and **Fig. 2b**, we can see that the vibration intensity increases the cartilage strength and the modulus of elasticity because vibration increases the friction forces in internal physiological bio-fluid occurring between the mutually contacted cartilage particles. Hence, viscosity increases in the internal bio-liquid, which implies that the elasticity modulus of the cartilage increases **[L. 11–12]**.

Medical practices demonstrate that it is possible to control the bio-liquid dynamic viscosity by means of the Hyalgan injection. The dose of the Hyalgan vaccine injected into bio-liquid, or synovial fluid, changes its dynamic viscosity **[L. 10]**. The bio-liquid after the Hyalgan injection exposes the particles of hyaluronic acid presented in **Fig. 3.**

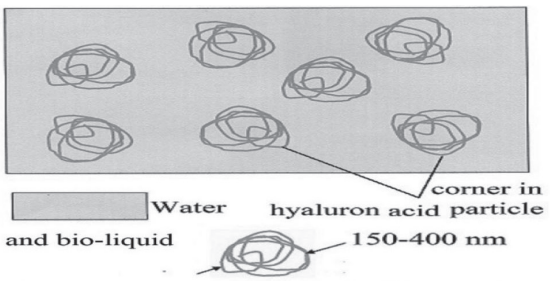

Fig. 3. Synovial liquid after Hyalgan Vaccine injected. Hyaluronic Acid particle has a characteristic corner which, during the flow, produces internal friction forces and thus, the bio-liquid's dynamic viscosity increases. Results obtained from the measurements by the Authors using Atomic Force Microscope

Rys. 3. Ciecz synowialna po wstrzyknięciu szczepionki Hyalganu. Cząsteczki kwasu hialuronowego mają widoczne charakterystyczne rożki, które podczas przepływu produkują dodatkowe siły tarcia wewnętrznego. Dlatego lepkość dynamiczna biocieczy ulega zwiększeniu. Wyniki uzyskane przez autorów przy użyciu AFM

The diameter of the Hyaluronic Acid particle varies from 150 to 400 nm. It is evident that Hyaluronic Acid has a particle with a characteristic corner, which during the flow of the liquid produces internal friction forces. Hence, it increases the sum of internal friction forces and this fact leads

to viscosity increments **[L. 3]**. These results have been obtained from the measurements performed by the Author using AFM. Moreover, this increases the lubricity i.e. the capability to create the bio-liquid superficial boundary layer **[L. 10–11]**.

Joint cartilage has tensile strength and it is manifested by the strength of the press & bending. Such features imply a biochemical interaction between collagen and proteo-glycans. Proteoglycans are a multi-molecular compound of protein. Collagen creates the collagen fibres of connective tissue. Collagen fibres are resistant to tension and not resistant to bending. Proteoglycans are resistant to press & bending, and they are not resistant to tension. Both components: mutually connected collagen fibres and proteoglycans, have a simultaneous resistance to tension and press & bending during the multiple joint motion **[L. 10–11]**.

A NEW VIEW OF THE NON NEWTONIAN BIO-LIQUID DYNAMIC VISCOSITY

A sketch of a theoretical model for bio-liquid dynamic viscosity

The lubrication problem is described in curvilinear orthogonal coordinates (a_i) for i = 1, 2, 3 by the following equations: an equilibrium of momentum equations, a continuity equation, an energy equation and a Young-Kelvin Laplace equation **[L. 4–5, 13]**. We take into account the following unknown functions **[L. 14]**: hydrodynamic pressure p [Pa], temperature T [K], bio-liquid or fluid velocity components v_i [m/s] for i = 1, 2, 3, the dynamic viscosity of synovial fluid $\eta_T(a_1, a_2, a_3)$ [Pas] and the joint gap height $\varepsilon_T(a_1, a_3)$ [m] **[L. 14–15]**. After term ordering, the expected function of the bio-liquid or fluid apparent dynamic viscosity η_T [Pa s] has the following form **[L. 4]**:

$$\eta_T(\alpha_1, \alpha_2, \alpha_3) = \eta_T(\mathrm{n}, p_H, T, \gamma, E) =$$
$$= \frac{\gamma_{\max}(p_H, \mathrm{We}) + k \cdot \left(A^{-1}\right) \cdot T \cdot \ln L}{\delta_v \cdot v_0} \left[1 + \delta_E\left(p_H, E\right) \cdot E^2\right] \left(\sqrt{\left(\frac{\partial v_{11}}{\partial a_{21}}\right)^2 + \left(\frac{\partial v_{31}}{\partial a_{21}}\right)^2} \right)^{n-1}, \tag{1a}$$

$$0 < L \equiv \frac{\left(\sqrt{L_k} + 1\right)^2}{\left(L_a + 1\right)\left(L_b + 1\right)} < 1, \quad L_a \equiv \frac{K_a}{a_H^+}, L_b \equiv \frac{a_H^+}{K_b}, L_k \equiv L_a L_b, \tag{1b}$$
$$\left(L_a + 1\right)\left(L_b + 1\right) > \left(\sqrt{L_k} + 1\right)^2.$$

We denote: k = 1.38054 · 10^{-23} [J/K] – Boltzmann constant, δ_v – dimensionless collage fibres concentration in biofluid, ($2 < \delta_v < 6$), δ_E[m^2/V^2] – experimental random coefficient of influence of electric intensity E [V/m] on the bio-fluid viscosity. From the basic equations and Formula (1a), it follows that the dynamic viscosity of the bio-liquid or synovial fluid is depended on the dimensionless power hydrogen ion concentration p_H, wettability *We* [Grade], and non-Newtonian properties manifested by the dimensionless flow index n whereas ($0.8 < n < 1.2$). For n = 1, we have Newtonian liquid. Furthermore, we denote: v_0 [m/s] – the characteristic value of bio-liquid velocity, v_{1i} for i = 1.3 – dimensionless bio-liquid velocity components, T [K] – temperature, $s = (N_A \cdot A)^{-1}$ [mol/m^2] – the concentration of PL particles, γ [J/m^2 = N/m] − interfacial energy, γ_{max} [N/m] − is the maximum interfacial energy of the lipid membrane, K_a [J] − acid equilibrium constant (2.58J) (this denotes how much energy is needed to stretch the bilayer), K_b [J] − base equilibrium constant (5.68 J) (this denotes how much energy is needed to bend or flex the bilayer), a_H [J] − protons energy activity, A [m^2] − the region of cartilage surface coated by PL molecules, $N_A = 6.024 \cdot 10^{23}$ − Avogadro number. Due to the presence of phospholipids bi-layers on the cartilage surface and the presence of lipo-somes, micelles, macromolecules and lamellar aggregates in the synovial fluid, this liquid has non-Newtonian especially pseudo-plastic properties **[L. 4–5]**.

General view of bio-liquid dynamic viscosity variations

By virtue of the measurements and computer calculations, we show a new extended description and interpretation of various influences on the variation of non-Newtonian pseudo-plastic bio-liquid dynamic viscosity in this intersection. Dynamic viscosity (Pas) of non-Newtonian pseudo-plastic bio-liquids increases vs:

1. Increments of pressure [N/m^2 = Pa],
2. Decrements of temperature from 316 K to 308 K (43°C, 35°C),
3. Decrements of Shear Rate **[L. 11]** from 1000 000 Hz to 10 Hz,
4. Decrements of the elasticity modulus **[L. 10]** during the rotating or linear motion of the superficial layer of cartilage surface which is by bio-liquid lubricated from 1000 MPa to 2 MPa,
5. Increments of the elasticity modulus **[L. 10]** during the squeezing motion of the superficial layer of cartilage surface which is by bio-liquid lubricated from 2 MPa to 1000 MPa,
6. Increments of variable electro-magnetic (EM) especially magnetic induction (MI) field from 10 to 30mT,
7. Increments of magnetic intensity **[L. 5]** in the interval from 40 kA/m to 100 kA/m,
8. Decrements of time **[L. 16]** [in years],
9. Increments of the characteristic value of acoustic emission intensity [W/m^2] **[L. 17]** in the level from 1 to 10B,
10. Increments from 2 to 4 and decrements from 12 to 4 of power hydrogen ion concentration, pH **[L. 4]**,
11. Increments of collagen fibre concentration **[L. 10]** in an interval from 100 to 100,000 mol/mm^3,
12. Decrements of cartilage surface wettability from 50° (hydrophilic) to 70° (hydrophobic) **[L. 18–19]**.

Dynamic viscosity of bio-liquid inflowing on bio-surface with wettability feature

Bio-liquid flows on a cartilage surface with a phospholipid bilayer (PL). By virtue of measurements and dynamic viscosity numerical calculations from Equation (1ab), we illustrate in **Fig. 4** that the absorbability (wettability) increments (from We = 70° → to We = 50°) of the cartilage surface imply bio-liquid or fluid dynamic viscosity decrements (from η = 0.50 Pas → to η = 0.40 Pas) **[L. 18]**.

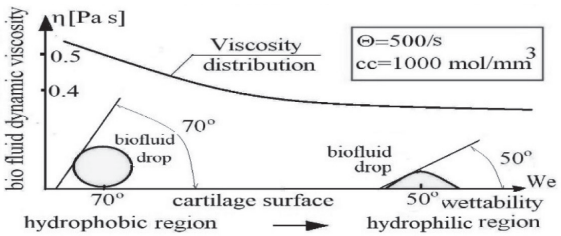

Fig. 4. Decreases of bio-fluid dynamic viscosity versus surface wettability increments (from hydrophobic We = 70° to hydrophilic region We = 50°). Horizontal wettability scale is presented in grades for the angle between the tangent line to the biofluid drop surface and the horizontal lubricated cartilage surface

Rys. 4. Spadek lepkości dynamicznej biocieczy wraz ze wzrostem nasiąkliwości biopowierzchni (od hydrofobicznej 70° do hydrofilnej We = 50°). Pozioma skala nasiąkliwości jest przedstawiona w stopniach dla kąta pomiędzy styczną do powierzchni biocieczy a poziomą powierzchnią smarowanej chrząstki

Figure 4 shows two drops of biofluid which constitute the rest on the horizontal cartilage surface.

- On the left side in **Fig. 4**, the spherical drop surface of the bio-liquid or bio-fluid has very small contact with the horizontal cartilage surface. Hence, the penetration → absorbability (wettability) of the biofluid into the cartilage surface is very small. In this case, the grade of the angle between the tangent line to the biofluid drop surface and the horizontal lubricated cartilage surface has the value of 70°. Hence, in this place, we have hydrophobic features of cartilage surface and in this point we denote wettability We = 70°.
- On the right side in **Fig. 4**, the parabolic drop surface of the bio-liquid or bio-fluid has very large contact with the horizontal cartilage surface. Hence, the penetration absorbability (wettability) of biofluid particles into the cartilage surface is very large. In this case, the grade of the angle between the tangent line to the parabolic biofluid drop surface and the horizontal lubricated cartilage surface has the value of 50°. Hence, in this place, we have hydrophilic features of cartilage surface and in this point we denote wettability We = 50°.
- Increments of the bio-surface wettability illustrated in **Fig. 4** denote the transformation from the hydrophobic (a small absorbability

bio-surface with 70°) to hydrophilic (large absorbability bio-surface with 50°) features.

- Experimental and calculated data presented in **Fig. 4** was obtained for a constant shear rate value of 500 Hz of the liquid flow and for a constant value of collagen fibre concentration in synovial liquid (bio-fluid) equal to cc = 1000 mol/mm^3. The cartilage surface coated with the PL is considered to be a bio-surface.

Dynamic viscosity of bio-liquid depended on collagen fibre concentration

By virtue of measurements and dynamic viscosity numerical calculations from Equation (1ab), we illustrate in **Fig. 5** that collagen fibre concentration increases from 100 to 100 000 mol/mm^3 in bio-liquid, then we have increments of bio-liquid dynamic viscosity from 0.3 Pas to 0.5 Pas **[L. 8]**, **[L. 10]**.

The aforementioned experimental data presented in **Fig. 5** was obtained for a constant shear rate value of 500 Hz for bio-liquid flow and for constant wettability We = 50° value, which determines the absorbability (wettability) of the cartilage surface. Moreover, the following are taken into account in the measurements: a phospholipid bilayer with an amino-group for pH from 2 to 4 (power hydrogen ion concentration), a constant value of temperature T = 310 K, interfacial energy from γ = 2.2 mJ/m^2 to γ = 3.5 mJ/m^2, and a constant value of liquid flow velocity v = 1.5 m/s.

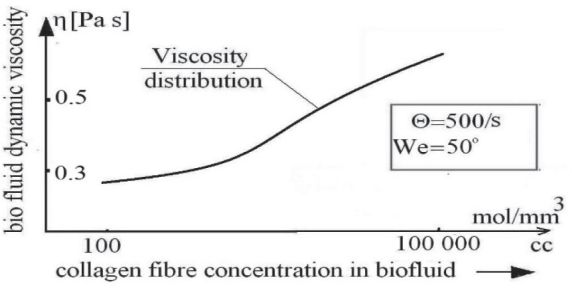

Fig. 5. Increases of bio-liquid or bio-fluid dynamic viscosity versus collagen fibre concentration increments obtained after AFM measurements and computer calculations (see Equation 1ab) taking into account phospholipid bilayer PL, the constant value of the shear rate of bio-liquid flow and the constant value of the wettability of cartilage surface

Rys. 5. Wzrost lepkości dynamicznej biocieczy ze wzrostem koncentracji włókien kolagenu na podstawie pomiarów AFM oraz obliczeń komputerowych (wzór 1ab), przy uwzględnieniu PL, oraz stałej wartości prędkości ścinania w przepływie cieczy a także stałej wartości nasiąkliwości powierzchni chrząstki

Dynamic viscosity of bio-liquid depended on the elasticity modulus of inflowed cartilage surface

By virtue of the measurements and numerical calculations from Equation (1ab) in Mathcad 15 Professional Program, in **Fig. 6**, we illustrate the bio-liquid dynamic viscosity variations depending on the elasticity modulus of cartilage **[L. 10]**. For the PL bilayer with PS and PC, and for lubrication by rotation, we observe that the bio-liquid or bio-fluid dynamic viscosity decreases if the elasticity modulus increases of the superficial layer of cartilage surface on which the bio-fluid flows. The aforementioned computational data presented in **Fig. 6** is obtained during the motion of rotation with an angular velocity from 0.1 to 1.5 1/s for:

- a power hydrogen ion concentration value pH = 9 in bio-liquid,
- a constant value of temperature T = 310 K,
- wettability We = 60° of the cartilage surface,
- the power value of acid equilibrium constant *pKa* = 2.58,
- the power value of base equilibrium constant *pKb* = 5.68,
- interfacial energy from γ = 1.5 mJ/m^2 to γ = 1.7 mJ/m^2 ,
- collagen fibre concentration in synovial liquid equal to cc = 1000 mol/mm^3.

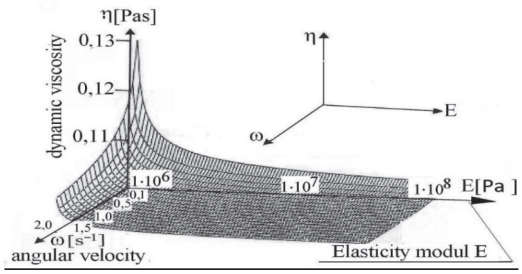

Fig. 6. Bio-liquid dynamic viscosity variations versus flow angular velocity [1/s] in lubrication by rotation and elasticity modulus [Pa] of the joint cartilage surface on which the lubricant liquid flows. Calculations performed for the constant value (pH = 9) of power hydrogen ion concentration in bio-liquid and the constant value of temperature T = 310 K, cartilage surface wettability We = 60° of the lubricated cartilage surface

Rys. 6. Zmiany lepkości dynamicznej biocieczy ze wzrostem prędkości kątowej [1/s] w smarowaniu rotacyjnym oraz ze wzrostem modułu sprężystości [Pa] powierzchni chrząstki stawowej, na której płynie ciecz smarująca. Obliczenia przeprowadzono dla stałej wartości (pH = 9) potęgi koncentracji jonów wodorowych w biocieczy w temperaturze T = 310 K przy nasiąkliwości powierzchni We = 60° smarowanej powierzchni chrząstki

To explain the phenomenon of liquid dynamic viscosity variations illustrated in **Fig. 6**, we present below the following reasoning. The increments of the E-(elasticity) modulus of the wall surface that restricted the gap imply the wall strength (resistance) increments, hence the decrements of the gap height are negligibly small in comparison with the places where the elasticity modulus and wall resistance were small, which gives the decrements of gap height. On the grounds of the abovementioned phenomenon, we obtain the following sequence of implications: E modulus increases → gap height decreases → flow speed increases → shear rate increases → viscosity decreases.

Dynamic viscosity of bio-liquid depended on the sound intensity of Acoustic Emission (AE)

At first, we must define some fundamental units of acoustic emission. The main unit is sound intensity denoted by J in W/m^2 and defined as the product of sound pressure p in Pa = N/m^2 and sound velocity v in m/s of the environment medium particle. Hence, the following formula **[L. 20]** is satisfied:

$$J = p \cdot v \tag{2}$$

The reference to sound intensity in air has the value: $J_0 = 10^{-12}$ W/m^2. We assume that the dimensionless, characteristic value of the acoustic intensity level has the form: $L_0 = 0.5 \ln (J/J_0)$. Taking the dimensionless value $J/J_0 = 10$ into account, we define the following essential sound units Bel in the form: 1B = 1 bel = 0.5 ln(10) = 1.1512….., and 1dB = 1 decibel = 0.1 B = 0.05 ln(10) = 0.111512… In acoustic emission therapy, the interval of the sound unit measured in decibels attain values from 0 to 100dB. The dimensionless might level of the acoustic emission (AE) therapy is defined as a fraction of the sound intensity for the actual bio-sample measured, to the maximum value of sound intensity J_{pmax} existing for a pathological bio-sample. The abovementioned level has the form: $L = J/ J_{pmax}$. The AE might level is directly proportional to the square of the AE wave amplitude.

If the sound intensity increases in the wave of acoustic emission, the contact between environment medium (air) particles increases. Hence, friction forces increase between contacting medium particles. Thus, the dynamic viscosity increases in the aforementioned medium (can be air or bio-fluid). This fact was proved in an experimental manner. In the following experiment, AE sound intensity values were measured and applied in bio-liquid inflowing on the cartilage sample. Hence, we have: J_s for a normal (sound) cartilage sample (2 mm ×2 mm), J_{ap} for an average pathological cartilage sample (2.4 mm ×2.5 mm) and J_{pmax} for a pathological cartilage sample (2.4 mm ×2.5 mm). On the grounds of abovementioned assumptions, we have the following AE might sound intensity levels **[L. 20–21]**:

$$L_s = J_s/ J_{pmax} = 0.209,\ L_{ap} = J_{ap}/ J_{pmax} = 0.827,\ L_{pmax} = J_{pmax} / J_{pmax} = 1.000 \tag{3}$$

All the measurements are performed using a mechanical sensor for: ● temperature 300 K, ● wettability We = 60^o of the cartilage surface, ● power hydrogen ion concentration value pH = 6 in synovial liquid, ● collagen fibre concentration in synovial liquid equal to cc = 100 mol/mm^3, ● average frequencies and amplitudes of AE waves equal to 20 kHz and 3 μm. For each lubricated sample, the value was measured simultaneously of synovial liquid shear rate flow Θ in Hz and lubricated liquid dynamic viscosity η in mPas. For the normal (sound), average pathological and pathological cartilage samples B. Ziegler **[L. 17**, **21–23]**, the following measurements data: flow shear rate in Hz, AE – sound intensity level in a dimensionless form (3), bio-liquid dynamic viscosity values in mPas presented in the following forms (4a, 4b, 4c):

$$\text{(normal cartilage) } \Theta = 800{,}000 \text{ Hz},\ L_s = 0.209 ,\ \eta = 150 \text{ mPa·s}, \tag{4a}$$

$$\text{(average pathological cartilage), } \Theta = 3{,}750\ 000\text{Hz},\ L_{ap} = 0.827,\ \eta = 125 \text{ mPa·s}, \tag{4b}$$

$$\text{(pathological cartilage), } \Theta = 3{,}750\ 000\text{Hz},\ L_{pmax} = 1.000,\ \eta = 150 \text{ mPa·s} \tag{4c}$$

- Taking into account the values measured obtained for normal and pathological cartilages (4a),(4c), it is easy to see that the flow shear rate increases, AE sound intensity level increases, dynamic viscosity of synovial liquid flow is constant.This fact is presented in **Fig. 7**.

Figure 7c shows that the constant value of the dynamic viscosity is a sum of viscosities η_{AE} and η_Θ. Viscosity η_{AE} increases from 40 mPas to the 90 mPas and it is caused by a dimensionless increase

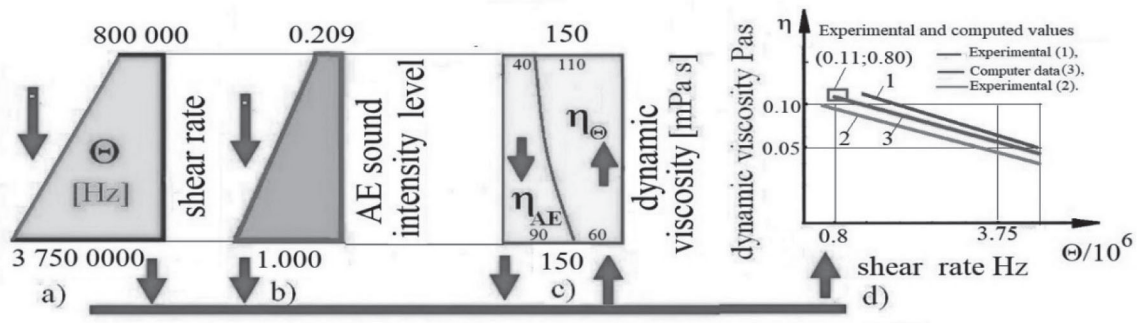

Fig. 7. The graphical form of the first step of measurements (4a), (4c): a) increases of the shear rate, b) increments of the AE sound intensity level, c) constant dynamic viscosity value, d) dynamic viscosity decrements versus shear rate

Rys. 7. Graficzna forma pierwszego zestawu pomiarów (4a), (4c): a) wzrost prędkości ścinania, b) wzrost poziomu intensywności dźwięku emisji akustycznej, c) stała wartość sumarycznej lepkości dynamicznej, d) spadek lepkości dynamicznej ze wzrostem prędkości ścinania

from 0.209 to 1.000 of the AE sound intensity level, cf. **Fig. 7b**. Viscosity η_Θ decreases from 110 mPas to 60 mPas and it is caused by an increase of the shear rate from 800,000Hz to 3,750,000 Hz illustrated in **Fig. 7**a and is presented in **Fig. 7d**.

- Taking into account the values measured obtained for average pathological and pathological cartilage (4b), (4c), it is easy to see that the flow shear rate is constant, AE sound intensity level increases, the dynamic viscosity of synovial liquid flow increases. This fact is presented in **Fig. 8**.

Figure 8c shows that the total value increments of the dynamic viscosity are a sum of the viscosity η_{AE} and η_Θ. Viscosity η_{AE} increases from 65 mPas to the 90 mPas and is caused by a dimensionless increase from 0.827 to 1.000 of the AE sound intensity level, cf. **Figure 8b**. Dynamic viscosity η_Θ has a constant value 60 mPas and is caused by the constant value of the shear rate equal to 3,750,000 Hz illustrated in **Fig. 8a** and is presented in the point depicted (0.06; 3.75), cf. **Fig. 8d [L. 21–23]**.

The graphical form of the first and second steps of measurements presented in **Fig. 7c** and **Fig. 8c** creates a probabilistic complete system of events **[L. 17]**. This fact leads to substantiation that the total value of dynamic viscosity η increases versus the increase of the AE sound intensity value. Hence, the proof presented had been completed.

- Considering dynamic viscosity η_{AE} provoked and caused by the proper AE sound intensity level presented graphically in **Fig. 7** and **Fig. 8**, we can illustrate in **Fig. 9** the average value of increases in the bio-liquid dynamic viscosity versus sound intensity increments.

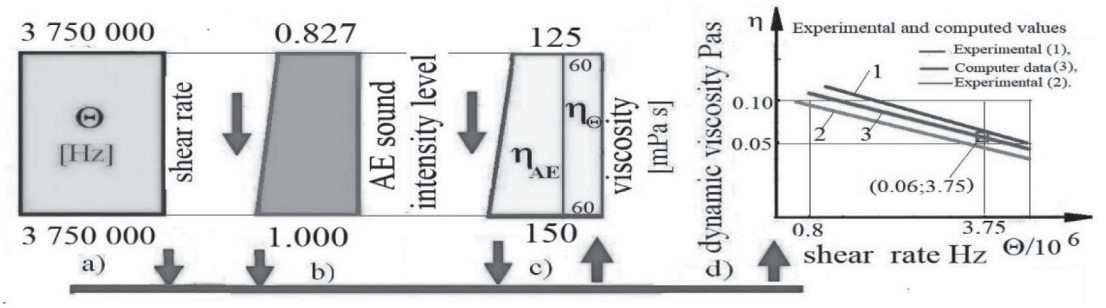

Fig. 8. The graphical form of the second step of measurements (4b), (4c): a) constant values of the shear rate, b) increases of the AE sound intensity level, c) increment values of the total dynamic viscosity, d) decreases of the dynamic viscosity versus shear rate increases

Rys. 8. Graficzna forma drugiego zestawu pomiarów (4b), (4c): a) stała wartość prędkości ścinania, b) wzrost poziomu intensywności dźwięku emisji akustycznej, c) wzrost sumarycznej wartości lepkości dynamicznej, d) spadek lepkości dynamicznej ze wzrostem prędkości ścinania

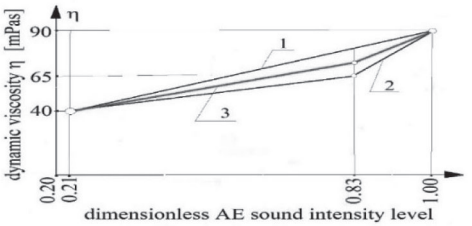

Fig. 9. Bio-liquid dynamic viscosity increments versus dimensionless AE sound intensity level increases 1 – according to results presented in Fig. 7, 2 – according to results shown in Fig. 8 and 3 – average values

Rys. 9. Wzrost lepkości dynamicznej cieczy biologicznej ze wzrostem bezwymiarowego natężenia dźwięku emisji akustycznej: 1 – według wyników pokazanych na rys. 7, 2 – według wyników zilustrowanych na rys. 8 oraz 3 – po uśrednieniu wartości

Dynamic viscosity of bio-liquid depended on the random joint gap height variations

By virtue of gap height density function measurements described in **[L. 4–5**, **11]** and after analytical, numerical Mathcad 15 Professional Program calculations for two kinds of phospholipids PS and PC, the following results were obtained presented as the random variations of synovial fluid dynamic viscosity in **Fig. 10a, 10b.** The dimensionless dynamic viscosity random quotient ξ_n, depicted in vertical axis in **Fig. 10a**, denotes the fraction of dynamic viscosity random effects (nominator) to the dynamic viscosity without random effects (denominator). For the f_N – density function measured (random increments dominate over decrements), **Fig. 10a** shows that the quotient ξ_n, of the dimensionless dynamic viscosity attains a decrement of 0.612 for PS, PC with probability P = 0.604, and it attains an increment of 1.388 with probability P = 0.729 for PS and with probability P = 0.788 for PC, in comparison with the dimensionless viscosity quotient ξ_n= 1, obtained without any random changes.

Fig. 10a illustrates bio-liquid dynamic viscosity increments vs. gap height random increments for the density function measured of the gap height and probability P. Inside the standard deviation interval on axis δ_1, we find the expected value: m_1 = 0.25 for corrected gap height 1.25 ε_T, with expected dynamic viscosity quotient increments which attain the value of 1.15 with probability P = 0.916 for PC, in comparison with the dynamic viscosity quotient ξ_n= 1, without any random effects. And we find the expected value: m_2 = 0.125 for corrected gap height 1.125 ε_T where the increments of the expected dynamic viscosity quotient attain the value of 1.09 with probability P = 0.937 for PS in comparison with the dynamic viscosity quotient without any random effects for ξ_n= 1, δ_1 = 0.

Fig. 10b was elaborated for the same density function. We show that in the radial clearance interval from 2 μm to 10 μm, the

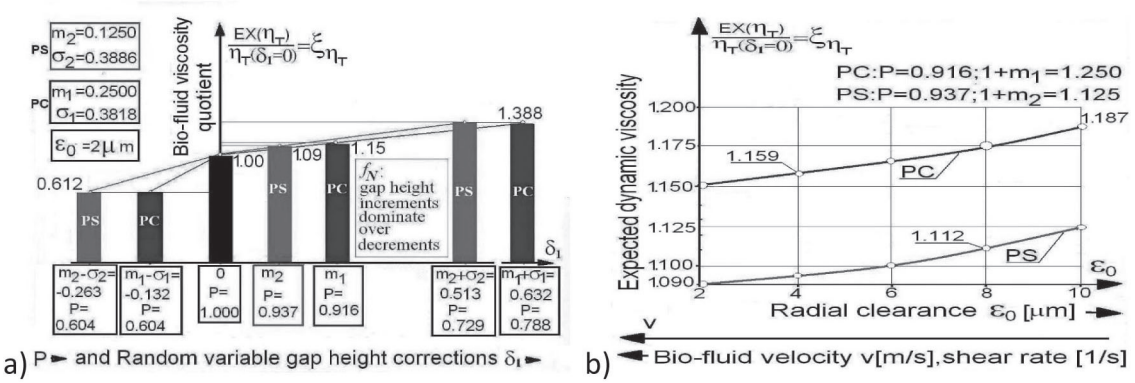

Fig. 10. Dimensionless random bio-fluid dynamic viscosity quotient ξ_n, for the density function measured of gap height in a spherical hip joint, a) versus random variable gap height corrections δ_1 and probability P, inside the standard deviation interval of gap height (1 + m – σ < 1 + m + σ) ε_T with expected value m and standard deviation σ for radial clearance 2 μm; b) versus radial clearance from 2 to 10 m, with constant probability P and constant expected values m_1, m_2 of gap height gap height for PC, and for PS

Rys. 10. Bezwymiarowe ilorazy losowych wartości lepkości dynamicznej ξ_n biocieczy dla pomierzonych losowych gęstości wysokości szczeliny sferycznego stawu biodra; a) jako funkcja losowo zmiennych korekt wysokości szczeliny δ_1 i prawdopodobieństwa P wewnątrz przedziału odchylenia standardowego wysokości szczeliny (1 + m – σ < 1 + m + σ)ε_T dla wartości oczekiwanej m i odchylenia standardowego σ przy luzie promieniowym 2 μm; b) jako funkcja luzu promieniowego od 2 do 10 μm, o stałym prawdopodobieństwie P oraz o stałych wartościach oczekiwanych m_1, m_2 wysokości szczeliny dla PC oraz dla PS

dimensionless random quotient ξ_n, of the expected value of bio-fluid dynamic viscosity increases from 1.15 to 1.19 with constant probability $P = 0.916$ and a constant expected value of gap height 1.25 ε_T for PC. Random dynamic viscosity quotient ξ_n, increases moreover from 1.09 to 1.13 with constant probability $P = 0.937$ and a constant expected value of gap height 1.125 ε_T for PS, in comparison with the dimensionless dynamic viscosity quotient without random effects for $\xi_n = 1$, $\delta_1 = 0$.

SYMPTOMS OF DISEASES AFTER BIO-LIQUID DYNAMIC VISCOSITY LOSS

Now we are presented various symptoms of diseases caused by the dynamic viscosity decrements of bio-liquid lubricants in bio-joints.

Arthritis and rheumatoid joint inflammation

Question: What fact enables us to straight or bend our fingers? Answer: Hydrodynamic pressure and load carrying capacity which is created in phalangeal joints!

Comment: Rheumatoid joint inflammation and arthritis increase the wettability We of the cartilage, decrease the concentration s of PL particles, decrease the collagen fibre concentration cc in bio-liquids lubricating surfaces of phalangeal joints and randomly decreases the clearance between joint cooperating cartilage surfaces. Hence, by virtue of the charts illustrated in **Fig. 4, Fig. 5** and **Fig. 10a, b** the dynamic viscosity decreases of synovial liquid in the phalangeal joint. Thus, on the grounds of the hydrodynamic theory of lubrication, we are going to the hydrodynamic pressure decrements and phalangeal joint load carrying capacity decrements. Hence, we have no sufficient forces and we cannot bend our fingers. After a long time of the duration of joint inflammation, finger curvature is fixed presented in **Fig. 11a, b** and clearance increments are fixed; cf. **Fig. 11c**. In **Fig. 11d**, we show the places of marrow structure changes in bone phalangeal after joint inflammation **[L. 10]**.

Fig. 11. Rheumatoid arthritis, joint inflammation: a) view of two pathological palms, b) X-ray photo of pathological joints in left and right palms, c) X-ray photo of end phase of palm degradation, d) internal changes in pathological bone molecular structure

Rys. 11. Reumatyczny artretyzm i zapalenie stawu: a) spojrzenie na dwie chore dłonie, b) zdjęcie Roentgena chorych stawów lewej i prawej dłoni, c) zdjęcie Roentgena końcowego stadium chorej dłoni, d) wewnętrzne zmiany w strukturze chorej kości stawowej

By virtue of the illustration presented in **Fig. 11** and the aforementioned descriptions, it follows that Rheumatoid Joint Inflammation (RJI) not only decreases the dynamic viscosity of synovial liquid in human joints but it also implies changes in bone marrow. Hence, chondrocytes occur in marrow that is to die during and after inflammation (see **Fig. 11d**). Thus, bending of human fingers is additionally immobilised.

In the first phase of inflammation disease, an effective increment of the dynamic viscosity of synovial liquid in the phalangeal joints gap can be attained by the therapy of (EM) especially variable (MI) field for 10mT with frequencies 15Hz once a day, 12 minutes per 21 days, cf. Eq. (1.1), Section 2.2 Point 6. Variable AE field can be applied, see **Fig. 9** for sound intensity level L = 0.83 with frequencies of 100 kHz and an amplitude of 9 μm.

What is preferred is the Hyalgan Vaccine injection in a dose of 2 mg/2 ml to deliver a Hyaluron Acid particle into the joint gap for the increments of synovial liquid dynamic viscosity.

Non-treated RJI causes the palm or limb amputation and, next, this fact implies an endoprosthesis implantation.

Comparison of diseases treated with bio-liquid dynamic viscosity enhancement

The therapy for enhancing the bio-liquid dynamic viscosity is applied in various diseases. For example, **Table 1** shows a possibility of a dynamic viscosity increase by the application of the AE sound intensity level L (see **Fig. 9**). Normal cartilage with small used places is treated with AE for L = 0.21 to obtain proper viscosity increments for the joint right functioning **[L. 21]**. And pathological cartilage with osteoporosis defects is treated with AE for L = 0.50 (see **Tab. 1**).

Table 1. Matrix of AE sound intensity level L applications for bio-liquid dynamic viscosity enhancements during the therapy of various diseases or cartilage defects

Tabela 1. Zestawienie poziomu L intensywności dźwięku emisji akustycznej AE dla podwyższania lepkości dynamicznej podczas terapi różnych schorzeń lub uszkodzeń chrząstki

Number of patients	Number of samples and the human joint	Applied level L of AE sound intensity waves	The average frequency of the AE waves	The average amplitude of the AE waves	Comparison of various diseases and cartilage defects
10	10 knee or hip	0.05	4 kHz	0.5 μm	Normal non-defective cartilage surface
29	29 hip	0.21	20 kHz	2 μm	Normal cartilage with small used places on the surface
10	10 knee and hip	0.39	40 kHz	3–4 μm	Pathological cartilage with a few arthritis defects on the external surface
10	10 knee	0.50	79 kHz	2–7 μm	Pathological cartilage with osteoporosis defects
10	10 knee	0.64	80 kHz	9 μm	Pathological cartilage with huge arthritis defects on the external and internal surface Layer
29	29 hip	0.83	100 kHz	9 μm	Pathological cartilage with average large defects caused by rheumatologic inflammation
29	29 hip or knee	1.00	150 kHz	10 μm	Pathological cartilage with very large defects caused by rheumatologic inflammation or arthritis defects on the external and internal surface layers

CONCLUSIONS

This paper indicates that the one of the main reasons of the loss of the human joint motion skill is an improper and low value of dynamic viscosity of bio-liquid lubricants, connected with a low hydrodynamic pressure and load carrying capacity.

This paper presents effective therapy methods to obtain a bio-liquid dynamic viscosity enhancement. These methods include: 1. Increasing of AE sound intensity level and AE field especially magnetic intensity and induction, 2. Increasing of collagen fibres concentration in bio-liquid joint lubrication. 3. Increasing of PL particles concentration in bio-liquid joint lubrication. 4. Adjusting dimensionless hydrogen ion concentration in bio-liquid lubricant to the value of pH = 4 for an optimum dynamic viscosity value. 5. Application of Hyaluronate Acid or a Hyalgan injection into the pathological gap joint.

DISCUSSION

This paper presents a new recent view in bio-tribology knowledge concerning the mutual connection between bio-lubricants dynamic viscosity and various symptoms of bio-joints diseases with numerous damages to bio-surfaces. The abovementioned connection process has an important meaning to the mutual influence of liquid dynamic viscosity on the wettability and other physical properties of lubricated bio-surface with a phospholipid bilayer (PL).

To the Author's best knowledge, the numerous previously experimental and theoretical studies in bio-tribology and bio-medical domain on the scope of bio-hydrodynamic human bio-joints lubrication have not focused to explain the connection between human joint skill and dynamic viscosity of the bio-liquid lubricating the cooperating cartilage surfaces. In this paper, the abovementioned problem was discussed. And, additionally, the methods are described for bio-liquid dynamic viscosity enhancement.

It is worth to note that the enhancement of bio-liquid lubricant dynamic viscosity to obtain load carrying capacity increments of human joints, resulting the increasing of the skill of limbs, is probably not unique but it is the major method of therapy of many human joints diseases.

To the Author's best knowledge, the aforementioned problem of an enhancement of bio-liquid dynamic viscosity has not been solved or elaborated in medical and tribology literature until this day.

REFERENCES

1. Andersen O.S., Roger E., et al.: Bilayer thickness and Membrane Protein Function: An Energetic Perspective. Annular Review of Biophysics and Biomolecular Structure, 201436 (1), pp. 107–130.
2. Bhushan B.: Handbook of Micro/Nano TribologySecond edCRC Press, Boca Raton, London, New York, Washington D.C. 1999.
3. Bhushan B.: Nanotribology and Nanomechanics of MEMS/NEMS and BioMEMS/BioNEMS materials and devicesMicroelectronic Engineering 2007, 84, pp. 387–412.
4. Wierzcholski K.: A New Progress in Random Hydrodynamic Lubrication for Movable Non-Rotational Curvilinear Biosurfaces with Phospholipid Bilayers, Lidsen Publishing Inc, Recent Progress in Materials 2021, volume 3, issue 2, pp. 1–38, DOI:10.21926/rpm.2102023, http://www.lidsen.com/journals/rpm/rpm-03-02-023.
5. Wierzcholski K., Miszczak A.: Estimation of Random Bio-Hydrodynamic Lubrication Parameters for Joints with Phospholipid Bilayers. Bulletin of Polish Academy of Sciences Technical Sciences, vol. 69 (1) e135834, DOI:10.24425/bpasts2021.135834.
6. Cwanek J.: The usability of the surface geometry parameters for the evaluation of the artificial hip joint wear.Rzeszów University Press, Rzeszów 2009.
7. Mow V.C., Ratcliffe A., Woo S.: Biomechanics of Diarthrodial Joints Springer Verlag, Berlin-Heidelberg New York 1990.
8. Wierzcholski K., Miszczak A.: Mathematical principles and methods of biological surface lubrication with phospholipids bilayers2019, www.elsevier.com.Biosystems, https://doi.org/10.1016/j.biosystems 2018.
9. Chizhik S., Wierzcholski K., Trushko A., Zhytkowa M., Miszczak Andrzej: Properties of cartilage on macro and nanolevel. Advances in Tribology, Hindawi Publishing Corporation, New York 2010, http://www.hindawi.com/journals/at/2010/243150/.
10. Wierzcholski K.: The Elements of Technical Biomechanics. Monograph, pp. 1–127, Published by K. Wierzcholski, Koszalin University of Technology, ISBN 978-83-923367-6-3, Koszalin 2011/2012.
11. Wierzcholski K.,Gospodarczyk J.: On Random Expected Values Variations of Tribology Parameters in Human Hip Joints Surfaces. Tribologia 3/2021, pp. 45–56, DOI: 10.5604/01.3001.0015.6898, ISSN 0208 7774.

12. Wierzcholski K.: Nanotribology impact of run-walk,electro-magnetic hydrodynamic human joint and skin lubrication on the slimming and metabolic process. Annals of Nanoscience & Nanotechnology 2017, vol. 1, issue 1, artic. 1, pp. 1–7, http://remedypublications.com/annals-of-nanoscience-and-namotechnology-articles/pdfs /folder/ annt-v1-id1001.pdf.
13. Wierzcholski K., Miszczak A.: Electro-Magneto-Hydrodynamic Lubrication. Open Physics, 2018, 16 (1), pp. 285–291.
14. Wierzcholski K.: Joint cartilage lubrication with phospholipids bilayer. Tribologia 2016, 2 (265), pp. 145–157.
15. Wierzcholski K.: Topology of calculating pressure and friction coefficients for time-dependent human hip joint lubrication, Acta of Bioengineering and Biomechanics 2011, 13 (1), pp. 41–56.
16. Wierzcholski K.: Time depended human hip joint lubrication for periodic motion with stochastic asymmetric density function. Acta of Bioengineering and Biomechanics 2014, 16 (1), pp. 83–97.
17. Ziegler B., Wierzcholski K., A new measurements method of friction forces regarding slide journal bearing by using AE. Tribologia 2010, 1(229), pp. 149–156.
18. Pawlak Z., Petelska A.D., Urbaniak W., Fusuf K.Q., Oloyede, A.: Relationship Between Wettability and Lubrication Characteristics of the Surfaces of Contacting Phospholipids-Based Membranes. Cell Biochemistry and Biophysics 2012, 65 (3), pp. 335–345.
19. Petelska A.D., Figaszewski Z.A.: Effect of pH on interfacial tension of bilayer lipid membrane. Biophysical Journal 2000, 78, pp. 812–817.
20. https://en.wikipedia.org/wiki/sound intensity.
21. Wierzcholski K.: Acoustic Emission Diagnosis For Human Joint Cartilage DiseasesActa of Bioengineering and Biomechanics 2015, vol. 17, No. 4, DOI:105277/abb-00256,pp.www.actabio.pwr.wroc.p, vol. 17, no. 4, pp. 139–148.
22. Ziegler B., Wierzcholski K., Miszczak A.:A new method of measuring the operating parameters of slide journal bearing by acoustic emission.Tribologia 2009, 6, (228), pp.165–174.
23. Ziegler B.: Application of acoustic emission to identification of lubrication conditions of slide journal bearing (Zastosowanie emisji akustycznej do identyfikacji warunków smarowania łożysk ślizgowych), Ph. DDissertation Thesis, Technical University Koszalin, 12 October 2010.